

EFFICIENCY POTENTIAL OF RGS SILICON FROM CURRENT R&D PRODUCTION

S. Seren¹, M. Kaes¹, G. Hahn^{1,2}, A. Gutjahr³, A. R. Burgers³, A. Schönecker³

¹ University of Konstanz, Department of Physics, 78457 Konstanz, Germany

² also with Fraunhofer Institute for Solar Energy Systems (ISE), Heidenhofstr. 2, 79110 Freiburg, Germany

³ ECN - Solar Energy, P.O. Box 1, 1755 ZG Petten, Netherlands

Tel: +49-7531-88-3386, Fax: +49-7531-88-3895. Email: sven.seren@uni-konstanz.de

ABSTRACT: Ribbon Growth on Substrate (RGS) is a low cost silicon ribbon material for photovoltaics. The RGS growth technique allows the direct growth of wafers with a very high production speed of one wafer per second. An industrial compatible cost effective screen printing process results in an efficiency of 13.1% for an untextured RGS cell. Based on this efficiency the silicon consumption per W_{Peak} for a 300 μm thick RGS wafer calculates to 5.4 g/W_{Peak} which is about 50% lower compared to standard block cast mc silicon material where a silicon loss of more than 50% appears due to ingot casting and wafering by wire saw. The silicon reduction is even more pronounced by the use of thinner RGS wafers. For efficiency demonstration a laboratory type high efficiency photolithography based process results in 14.4% efficiency on smaller cell size, which is the highest solar cell efficiency reached on RGS silicon so far. In this paper the applied cell processes as well as cell results are discussed by means of spectral response as well as spatially resolved LBIC measurements showing the characteristics of this multi-crystalline silicon ribbon material.

Keywords: Ribbon Silicon, Passivation, Hydrogen

1 INTRODUCTION

This paper focuses on latest solar cell results reached on a silicon ribbon material currently produced for research: Ribbon Growth on Substrate (RGS [1,2]) The RGS production principle shown in Figure 1 allows the direct growth of silicon wafers ready for solar cell processing without any aftertreatment such as wire-sawing or laser-cutting with a very high production speed of one wafer per second.

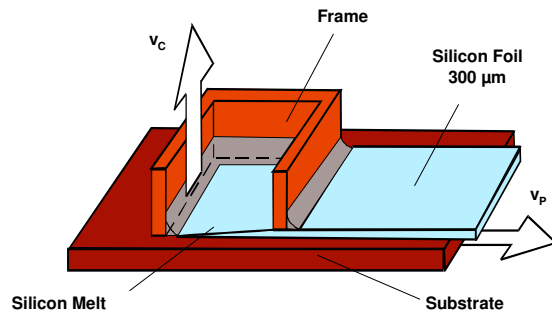


Figure 1: Principle of the RGS wafer production technique.

Substrate plates are pulled underneath the molten silicon inside a casting frame. The wafer crystallizes on the reusable substrate, which absorbs the crystallization heat. Decoupling of crystallization and pulling direction results in the very fast pull speeds in combination with moderate crystallization velocity.

RGS wafers were up to now produced by a laboratory scale R&D machine by ECN. The gained experience was introduced in a totally new designed RGS wafer casting machine which is being assembled at RGS Development B.V. at the moment. Until first wafers will be produced by the new machine within this year, RGS wafers of the R&D machine were processed to solar cells demonstrating the potential of the material.

The material is investigated in terms of solar cell processing and characterisation. In consequence of the material production principle the throughput is very high compared to other silicon ribbon materials like String Ribbon or EFG [3]. However, the crystal quality suffers from higher crystal defect densities such as dislocations, grain boundaries or impurities incorporated by the crucible, casting and substrate materials which limits the charge carrier lifetime of the material. This material limitation can be partially compensated by gettering and hydrogenation during solar cell processing [4]. Two different types of solar cell processes were applied to RGS silicon. A laboratory type high efficiency photolithography based cell process as well as an industrial-type screen printing firing through SiN process. The high efficiency process demonstrates the efficiency potential of the RGS material on small cell sizes whereas the screen printing process demonstrates the applicability of RGS wafers for larger scale industrial processing.

2 SOLAR CELL PROCESSING

RGS wafers are currently produced by a laboratory scale R&D machine at ECN and cells presented in this paper are processed at the University of Konstanz (UKN).

For efficiency demonstration a photolithography based cell process was chosen. The high efficiency process (Figure 2, right) includes a mechanically levelling of the uneven wafer front side using a wafer dicing saw in combination with a special planarisation tool. The planarisation is applied only to thick RGS wafers whereas thin RGS wafers show an almost flat wafer surface and can be processed without planarisation. After an acidic removal of defect-rich surface layers a 80 Ω/sq . emitter diffusion follows. For BSF formation Al is screen printed on the cell's backside, alloyed and subsequently chemically removed. The emitter is passivated by a SiN layer which additionally provides hydrogen for passivation of bulk defects during BSF

alloying. Front contact formation is realised by photolithography and back contact formation by evaporation of Al. Further on, the conductivity of the front contact metallisation is improved by Ag plating. After cell definition by dicing ($2 \times 2 \text{ cm}^2$), contact annealing and additional hydrogenation is performed in a microwave induced remote hydrogen plasma (MIRHP) reactor. Finally a double layer antireflective coating is realised by evaporation of MgF_2 .

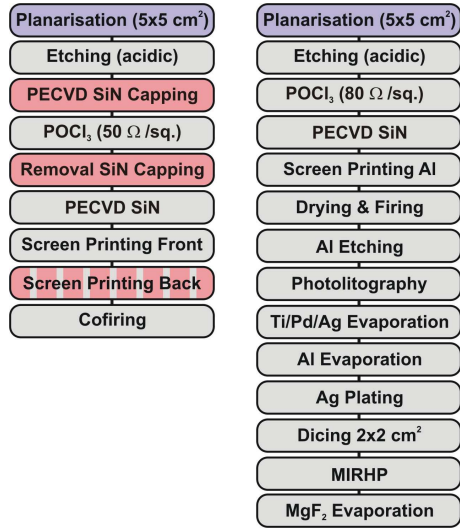


Figure 2: Solar cell processes applied to RGS. Left: Industrial-type firing through SiN screen printing process. Right: Photolithography based high efficiency process including screen printed Al BSF, hydrogenation and double layer antireflective coating (DARC).

The applied screen printing process (Figure 2, left) implies the same wafer pre-treatment as the high efficiency process (planarisation only for thick RGS wafers, acidic removal of defect rich surface layers). A single side POCl_3 emitter diffusion realised by a SiN capping layer in combination with an open rear side metallisation by screen printing of an Al grid pattern prevents process induced shunting [5,4].

During both cell processes phosphorus and aluminium gettering respectively takes place. Further on, an effective passivation of bulk defects by hydrogen originating from the hydrogen-rich SiN layer is involved in both cell processes as well. Thus, low as-grown minority carrier lifetimes are strongly improved by a factor of 10 as determined by μPCD lifetime measurements before (average $\mu = 0.5 \mu\text{s}$) and after (average $\mu = 5\mu\text{s}$) solar cell processing [4].

3 CELL RESULTS

According to the solar cell processes shown in Figure 2, RGS wafers with different as grown thicknesses were processed. The wafer thickness shown in Table I refers to the wafer thickness after the mechanical planarisation for the thicker RGS wafers ($> 200 \mu\text{m}$). The thin RGS wafers are flat enough to be processed without a planarisation step due to different crystallization conditions for the growth of thin RGS wafers.

Table I: IV data of the best solar cells processed at UKN from actual RGS material according to the cell processes presented in Figure 2. Cell sizes are $2 \times 2 \text{ cm}^2$ for the high efficiency process and $5 \times 5 \text{ cm}^2$ for the screen printing process, respectively.

RGS cell process	V_{oc} [mV]	J_{sc} [mA/cm^2]	FF [%]	η [%]
as grown wafer thickness $\sim 300 \mu\text{m}$				
high eta	596	30.6	79.1	14.4*
screen printing	591	29.1	75.8	13.1*
as grown wafer thickness $\sim 210 \mu\text{m}$				
high eta	584	29.6	75.4	13.0
as grown wafer thickness $\sim 130 \mu\text{m}$				
high eta	580	29.0	69.2	11.6
screen printing	568	25.9	71.6	10.6

The IV data of the solar cells marked with an asterisk have been independently confirmed by the ISE CalLab (high eta cell process) and the European Solar Test Installation (ESTI) of the Joint Research Centre (JRC) of the European Commission (screen printing process), respectively. The efficiency of 14.4% presented in Table I for the photolithography based process is the highest efficiency reached on RGS silicon so far. For the screen printing process 13.1% is the highest efficiency reached on RGS for an untextured solar cell with a single layer antireflective coating (SiN).

Latest RGS production experiments enabled the growth of very thin wafers with a thickness in the $130 \mu\text{m}$ range, which could be processed to solar cells using the screen printing process as well as the high efficiency process without major adaptations. The encouraging first results are 11.6% for the photolithography based and 10.6% efficiency for the screen printing process, respectively. Further gain in efficiency is expected if the cell processes are adapted to the attributes of the thin material. This assumption is confirmed by comparing the different cell efficiencies for the different wafer thicknesses of the high eta solar cell process presented in Table I. The cell efficiency decreases with decreasing short circuit current density as a result of the reduced absorption for the reduced wafer thickness. Further on, the open circuit voltage decreases with decreasing wafer thickness indicating a lower crystal quality of the thin RGS wafers maybe in combination with a limiting back surface recombination velocity for the fully covering Al BSF. However, assuming a constant minority charge carrier lifetime independent of the wafer thickness the decreased absorption of thin RGS wafers could be compensated by light confinement as a result of a surface texture in combination with an effective backside reflector.

4 SILICON CONSUMPTION PER $\text{WATT}_{\text{PEAK}}$

Based on the efficiency of 13.1% presented in Table I the silicon consumption per $\text{Watt}_{\text{peak}}$ for a $300 \mu\text{m}$ thick RGS wafer calculates to $5.4 \text{ g}/\text{W}_{\text{peak}}$. This advantageous value is enabled by the optimum silicon usage of the RGS technique in contrast to standard block cast mc silicon material where a silicon loss of more than 50%

appears due to ingot casting and wafering by wire saw. Compared to the silicon consumption per $\text{Watt}_{\text{peak}}$ for standard mc material (wafer thickness $250\ \mu\text{m}$, solar cell efficiency 15%) of $10.5\ \text{g}/\text{W}_{\text{peak}}$ [6] the RGS technique allows power generation with roughly half the amount of silicon input. Further on, starting from the actual result of the screen printing process for the $130\ \mu\text{m}$ thick RGS solar cell, a silicon consumption of only $2.9\ \text{g}/\text{W}_{\text{peak}}$ calculates. This indicates that with thin RGS material the silicon usage could be lowered by a factor of 3.6 or 72%, respectively, compared to standard mc material.

5 CHARACTERISATION

By comparing the IQEs of RGS solar cells processed from thick RGS material according to the two cell processes presented in Figure 2, a difference in the short wavelength range due to the differently doped emitters can be seen (black curves in Figure 3 and Figure 4). The same holds for the thin RGS solar cells (green curves in Figure 3 and Figure 4), demonstrating the loss in J_{sc} for the screen printed cells due to the enlarged dead layer as a result of the higher doped emitter.

The IQEs of the thin RGS solar cells show a lower material quality as is demonstrated by the reduced calculated diffusion lengths. This might be a result of the RGS crystal growth process, which is yet not optimized for casting of thin RGS material and possibly the influence of rear side recombination becoming important for thin wafers.

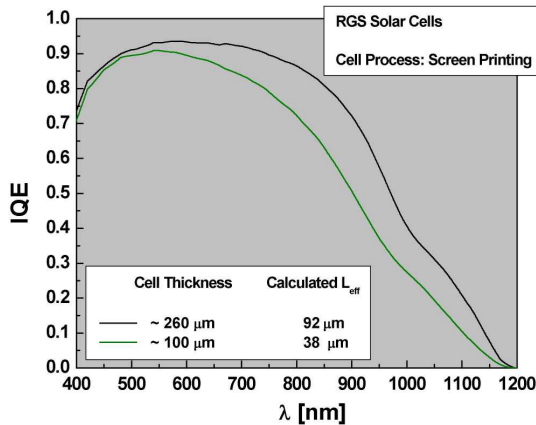


Figure 3: Internal quantum efficiency of solar cells processed from thick and thin RGS wafers according to the screen printing cell process shown in Figure 2.

Further on, the etching depth during the acidic removal of defect-rich surface layers was reduced for processing of thin RGS wafers which results most probably in a remaining fraction of disturbed crystal quality on the wafer front and substrate side lowering diffusion length and emitter quality. The latter effect is confirmed by the lowered FFs of the thin compared to the thick solar cells for the high efficiency and the screen printing process as well.

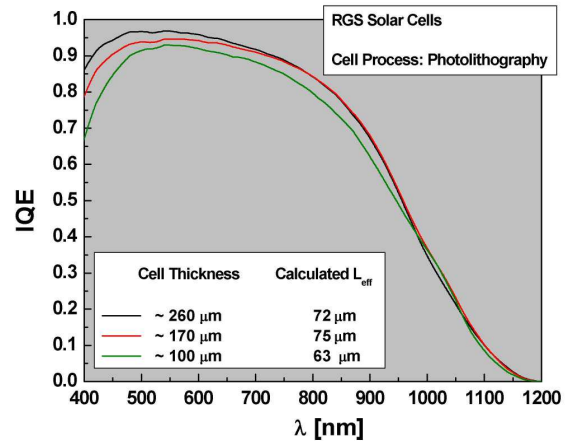


Figure 4: Internal quantum efficiency of solar cells processed from different thick RGS wafers according to the photolithography based cell process shown in Figure 2.

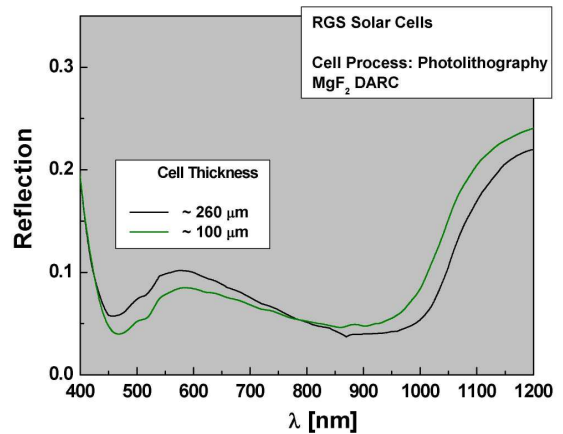


Figure 5: Reflection curves of two of the RGS solar cells as presented in Figure 4 (photolithography based cell process including a SiN / MgF₂ DARC).

The reflection curves for RGS solar cells processed from wafers with different thicknesses (photolithography based cell process including SiN / MgF₂ DARC) shown in Figure 5 demonstrate the lowered absorption in the long wavelength range for the thin RGS cell. Light confinement by surface texturing should lower the long wavelength reflection further, resulting in an enhanced J_{sc} . The reduced reflection of the thin cell in the short wavelength range is a result of a higher index of refraction of the deposited SiN layer.

The slightly reduced material quality of the thin RGS material can be observed in LBIC measurements as well. Figure 6 shows two LBIC mappings at a wavelength of 980 nm for the same cells as presented in Figure 4. The thin cell (Figure 6, right) shows on the left cell side (marked with arrows) an area of reduced internal quantum efficiency which is a result of a missing BSF as well as a missing Al gettering during BSF formation. Screen printing of Al was not performed in this area and thus the beneficial effect of the BSF to lower the recombination velocity of minority charge carriers is missing. In combination with an enhanced recombination

rate in areas of ungettered impurities in the crystal volume a lowered IQE signal and thus J_{sc} results.

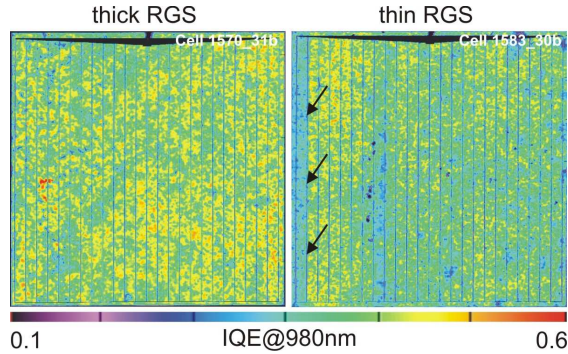


Figure 6: LBIC mappings of the same RGS solar cells as presented in Figure 4 and Figure 5 (photolithography process). The line marked with arrows in the right measurement indicates the range of Al screen printing.

6 OXYGEN CONTENT

Previous experiments showed that RGS material with high interstitial oxygen content $[O_i] (> 10^{18} \text{ cm}^{-3})$ resulted in limited solar cell efficiencies. It could be shown, that this effect is attributed to enhanced recombination at several oxygen related defects such as oxygen precipitates as well as New Donors, which form during wafer production or high temperature solar cell processing steps [7]. The high oxygen content also caused an extremely slow reaction of the RGS material to hydrogen passivation [8]. In order to overcome both limitations, the RGS wafer manufacturing process was improved which enabled the processing of RGS wafers with lower oxygen contents down to $4 \times 10^{17} \text{ cm}^{-3}$ [9]. These concentrations are comparable to standard cast multi-crystalline material.

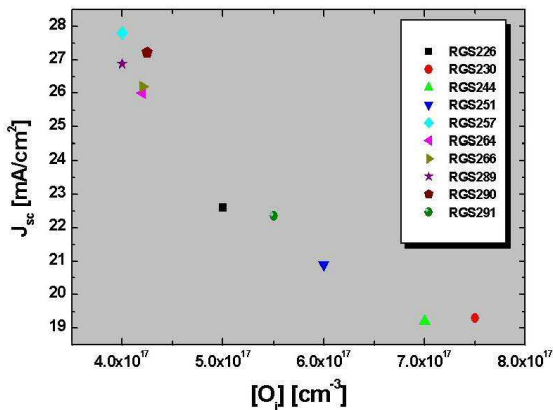


Figure 7: Dependence of J_{sc} on $[O_i]$ for solar cells produced from various RGS production runs (screen printing process). Shown are average J_{sc} values of the respective solar cell processing runs.

Figure 7 shows a clear correlation between lower interstitial oxygen concentrations of the as-grown wafers and higher J_{sc} values of the processed solar cells (screen printing process). Furthermore it was found, that a lower oxygen concentration results besides a faster

hydrogenation in larger diffusion lengths [10]. This effect is demonstrated in Figure 8 where two LBIC measurements of solar cells are shown (photolithography based cell process) which were processed from RGS material which differ in the interstitial oxygen concentration of about one order of magnitude. The IQE signal for the RGS cell processed from the low oxygen material is significantly enhanced (Figure 6, right).

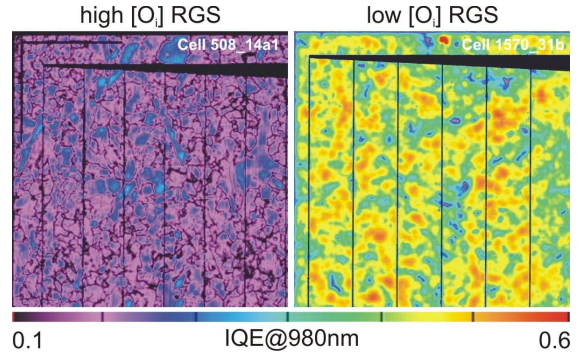


Figure 8: LBIC maps of two RGS solar cells (photolithography based cell process) from RGS wafers with different interstitial oxygen concentrations. The right mapping is a high resolution detail (upper left corner) of the cell shown in Figure 6, left.

In order to enhance the diffusion length of low oxygen RGS material further, besides gettering and hydrogenation as well as the avoidance of processing induced shunts [5,4] crystallographic investigations are currently performed concerning the influence of the grain size and the grain boundaries on the diffusion lengths of the RGS material. With lower oxygen concentrations the recombination activity of the grain boundaries is found to be reduced due to the lowered concentration of oxygen related defects decorating grain boundaries.

Compared to the high oxygen RGS cell (Figure 6, left), the low oxygen RGS cell (Figure 6, right) shows a pronounced structure of local areas of high IQE. To correlate the local grain size and crystal structure variations with the corresponding local material quality is subject of current investigations.

7 SUMMARY

Solar cells were processed from RGS material with different wafer thicknesses. Two different cell processes were used: an industrial-type screen printing process and a photolithography based high efficiency cell process to demonstrate the efficiency potential of the material. For both approaches the highest efficiencies published so far could be achieved. For wafer thicknesses of approximately $300 \mu\text{m}$ cell efficiencies of 14.4% and 13.1% resulted for the high eta cell process and the screen printing process, respectively. $100 \mu\text{m}$ thin RGS solar cells reached efficiencies of 11.6% and 10.6%, respectively, without major adaptations in the cell processes indicating potential for efficiency enhancing optimizations. Additionally, it was found that thin RGS material can be processed without a mechanical planarisation of the wafer surface which simplifies solar cell processing.

An estimation concerning the silicon consumption per W_{peak} based on the presented cell data showed a silicon reduction potential of about 50% for thick RGS and even 72% for thin RGS material.

Compared to solar cells processed from thick RGS material, thin RGS solar cells showed reduced internal quantum efficiencies as measurements and calculated diffusion lengths revealed. This is most probably due to the RGS crystal growth process, which is yet not optimized for casting of RGS wafers with such reduced thicknesses. Further on, the beneficial effect of Al gettering and the presence of a Al BSF could be visualized by a LBIC mapping of a thin RGS solar cell with a missing screen printed Al at the edge of the cell.

The detrimental effect of high interstitial oxygen concentrations on solar cell performances was demonstrated in terms of short circuit current densities of solar cells processed from RGS material containing different oxygen concentrations as well as by spatially resolved IQE measurements.

8 OUTLOOK

First promising results of thin RGS solar cells processed from RGS wafers with a thickness of only about 100 μm were obtained without major adaptations of the cell processes to meet the characteristics of the reduced wafer thickness. In future experiments for both processes (screen printing and photolithography based) the etching depth for the acidic removal of defect rich surface layers has to be optimised in order to establish emitter structures on crystal areas without defect-rich layers.

With a cell thickness approaching the diffusion length, dielectric passivation of the cell backside becomes important in order to reduce surface recombination velocity on the cell backside and thus increasing efficiency. Thus, cell designs suited for the thin RGS material have to be investigated.

To meet the lowered absorption as a result of the reduced cell thickness, light confinement has to be guaranteed by the application of a suitable surface texture. If a surface texture is included in cell processing J_{sc} should be enhanced further.

The most significant improvement in cell performance is expected due to material quality improvements as a result of wafer production in thermal equilibrium with a new, totally rebuilt production facility operating continuously which is built up at RGS Development B.V. at the moment.

9 ACKNOWLEDGEMENTS

Part of this work was funded by the EC in the RGSells (ENK6-CT-2001-00574) and the CrystalClear (SES6-CT-2003-502583) project. The content of this publication is the responsibility of the authors.

The RGS wafer manufacturing process development is carried out in the RGSolar project supported by the EET programme under EETK 03023.

10 REFERENCES

- [1] H. Lange, I. A. Schwirtlich, *Ribbon Growth on Substrate (RGS) - A new approach to high speed growth of silicon ribbons for photovoltaics*, J. Cryst. Growth, 104 (1990) 108
- [2] G. Hahn, A. Schönecker, *New crystalline silicon ribbon materials for photovoltaics*, J. Phys.: Condens. Matter 16 (2004) R1615-R1648
- [3] M. J. Kardauskas, M. D. Rosenblum, B. H. Mackintosh, J. P. Kalejs, *The coming of age of a new PV wafer technology – some aspects of EFG polycrystalline silicon sheet manufacture*, Proc. 25th IEEE PVSEC, Washington D.C. 1996
- [4] S. Seren, G. Hahn, A. Gutjahr, A. R. Burgers, A. Schönecker, *Ribbon Growth on Substrate - A Roadmap to higher Efficiencies*, Proc. 21st EU PVSEC, Dresden 2006
- [5] A. Burgers, A. Gutjahr, L. Laas, A. Schönecker, S. Seren, G. Hahn, *Shunt free solar cells on RGS wafers*, Proc. 4th WCPEC, Waikoloa, 2006
- [6] G. Hahn, S. Seren, M. Kaes, A. Schönecker, J. P. Kalejs, C. Dubé, A. Grenko, C. Belouet, *Review on Ribbon Silicon Techniques for Cost Reduction in PV*, Proc. 4th WCPEC, Waikoloa, 2006
- [7] D. Karg, A. Voigt, J. Krinke, C. Hässler, H.-U. Hoefs, G. Pensl, M. Schulz, H. P. Strunk, *Formation and annihilation of new donors in ribbon growth on substrate silicon*, Solid State Phenom. 67/68 33, 1999
- [8] G. Hahn, D. Karg, A. Schönecker, A. R. Burgers, R. Ginige, K. Cherkaoui, *Kinetics of Hydrogenation and Interaction with Oxygen in crystalline Silicon*, 31st IEEE PVSC, 2005, Lake Buena Vista
- [9] G. Hahn, S. Seren, D. Sontag, A. Gutjahr, L. Laas, A. Schönecker, *Over 10% efficient Screen-printed RGS Solar Cells*, Proc. 3rd WCPEC, Osaka, 2, 1285-1288, 2003
- [10] S. Seren, G. Hahn, A. Gutjahr, A. R. Burgers, A. Schönecker, *Screen-Printed Ribbon Growth on Substrate Solar Cells approaching 12% Efficiency*, Proc. 31th IEEE PVSC, Lake Buena Vista, 1055-1058, 2005